A calorimetric study on the configurational enthalpy and low-energy excitation of ground amorphous solid and liquid-quenched glass of 1, 3, 5-tri-α-naphthylbenzene



1996 J. Phys.: Condens. Matter 8 245

(http://iopscience.iop.org/0953-8984/8/3/005)

J. Phys.: Condens. Matter **8** (1996) 245–255. Printed in the UK

# A calorimetric study on the configurational enthalpy and low-energy excitation of ground amorphous solid and liquid-quenched glass of 1, 3, 5-tri-$\alpha$-naphthylbenzene

Itaru Tsukushi†, Osamu Yamamuro†, Tomoko Ohta†, Takasuke Matsuo†, Hideyuki Nakano‡ and Yasuhiko Shirota‡

† Department of Chemistry and Microcalorimetry Research Centre, Faculty of Science, Osaka University, Toyonaka, Osaka 560, Japan

‡ Department of Applied Chemistry, Faculty of Engineering, Osaka University, Suita, Osaka 565, Japan

Received 3 August 1995, in final form 2 November 1995

**Abstract.** An amorphous solid of 1, 3, 5-tri-$\alpha$-naphthylbenzene (TNB) was prepared by grinding the crystalline sample with a vibrating mill. Heat capacities of the ground amorphous solid (GAS), liquid-quenched glass (LQG) and crystal of TNB were measured with an adiabatic calorimeter in the temperature range 10–330 K for the GAS and 5–370 K for the LQG and crystal. The heat capacities of the LQG and GAS were 0.5–1% larger than that of the crystal. The heat capacity of the GAS agreed with that of the LQG between 30 and 330 K but was 1–4% larger than that of the LQG below 30 K. The heat capacity difference in the low-temperature region can be attributed to the difference in *low-energy excitation* which is known as a universal property of amorphous materials. A glass transition occurred at 342 K for the LQG. For the GAS, however, a large exothermic effect due to crystallization appeared from 315 K, which is 25 K lower than $T_g$ of the LQG. The configurational enthalpy of GAS determined from the enthalpy of crystallization was much larger than that of the LQG. This result indicates that the structure of the GAS is much more disordered and strained than that of the LQG.

## 1. Introduction

Amorphous solids are usually prepared by quenching their liquids or depositing their vapours on a cold substrate [1–3]. These procedures are based on rapid removal of the kinetic energy of the constituting entities. Recently, great attention has been paid to solid-state amorphization [4–6]. This is a process that takes an opposite approach to the conventional procedure, i.e., supplying energy to disturb an equilibrium crystal and freeze it in an energized metastable amorphous state. Most of the studies done so far have been for binary alloys of transition metals (Ni, Zr, etc) [7] and inorganic compounds ($SiO_2$, Se, etc) [8]. Mechanical grinding in a ball mill and irradiation with high-energy electron or neutron beams are commonly used techniques for solid-state amorphization. At present the amorphization process itself and the possible structure difference between the amorphous states obtained by these techniques and the traditional ones are the centres of interest. The x-ray and neutron diffraction and EXAFS techniques have been employed in these studies.

Recently, we have found that several organic molecular crystals can be amorphized by mechanical grinding using a vibrating mill [9–11]. The x-ray diffraction experiments showed that all of these ground amorphous solids (GAS) exhibit halo patterns similar to those of

0953-8984/96/030245+11$19.50  

the liquid-quenched glasses (LQG). In differential scanning calorimetry (DSC) for GAS samples, glass transitions appeared at the same glass transition temperatures as for LQGs. However, different behaviour was found in GAS and LQG of tri-*O*-methyl-$\beta$-cyclodextrin (abbreviated as TMCD) in a more detailed experiment using an adiabatic calorimeter [12]. The GAS sample released a configurational enthalpy twice as large as that for the LQG over an unusually wide temperature range below $T_g$. This result indicates that the GAS is more disordered and strained than the LQG.

In the present study, we have measured the heat capacities and enthalpy relaxation of 1, 3, 5-tri-$\alpha$-naphthylbenzene ($C_{36}H_{24}$, abbreviated as TNB) in the forms of GAS, LQG and crystal using an adiabatic calorimeter. TNB is a propeller-like molecule composed of a benzene core and three naphthalene blades as shown in figure 1. The blades are inclined to the molecular plane at a certain angle. The molecules exist in the right screw and left screw in an even ratio, though no conformational change occurs in the temperature range of current interest [13]. This molecule has an exceptionally simple structure (symmetry: $C_3$) and small molecular weight ($M = 456.6$) among the organic molecules whose crystals can be amorphized by mechanical milling. TNB is known as a popular glass-forming molecule. Physical properties of TNB LQG have been studied in some detail [13–20]. Among them are the thermal properties obtained from DSC [15, 18]. No physical properties of the TNB GAS have been studied so far.

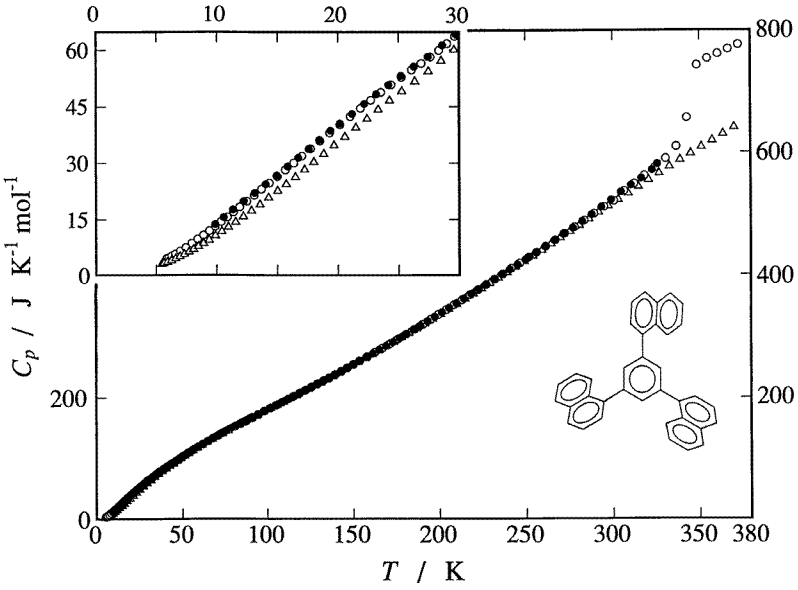


**Figure 1.** Heat capacities of TNB. Open circles: LQG; closed circles: GAS; triangles: crystal.

The main purpose of this work is to investigate the enthalpy difference between the TNB GAS and LQG and to compare the result with that for TMCD [12]. Because of the different molecular structures, the comparison may allow us to discuss the relative importance of the roles played by the inter- and intramolecular degrees of freedom in determining amorphous properties of molecular solids. Another purpose of this study is to investigate the heat capacity difference between the GAS and LQG in the low-temperature region. Anomalous (non-Debye) heat capacities of amorphous solids (for $T < 20$ K), originating from some *low-energy excitation*, is now believed to constitute a characteristic and universal property

of amorphous materials [21]. It is currently of interest to study the origin of the low-energy excitation and its dependence on the disorder and strain in the structure of the amorphous substances. Mechanical milling is an ideal method by which to prepare highly disordered and strained amorphous solids that may differ from LQG in various respects.

## 2. Experimental procedure

### *2.1. Sample*

TNB was prepared according to the method described in the literature [22] with a little modification: a mixture of $\alpha$-acetonaphthone (250 g, 1.47 mol), aniline (125 g, 1.34 mol), and aniline hydrochloride (10 g, 0.077 mol) was heated at 175 °C for 2 h under nitrogen atmosphere. After the aniline was removed, 150 ml of glacial acetic acid was added and the reaction mixture was refluxed for 2 h. The resulting tarry product was extracted with $CHCl_3$, washed successively with water, aqueous sodium hydrogen carbonate and water, and dried over $Na_2SO_4$. After the solvent was evaporated, the residue was chromatographed over neutral alumina (70–230 mesh, MERCK) using a mixed solvent of chloroform and hexane (1:4) as an eluent. The first portion gave TNB (yield 29.6 g, 13.2%), which was purified by recrystallization from a mixed solvent of chloroform and hexane, followed by heating at $\simeq$100 °C under reduced pressure. The values obtained by elemental analysis were C: 94.64; H: 5.22%. The values calculated for $C_{36}H_{24}$ were C: 94.70; H: 5.30%.

About 2.4 $cm^3$ (3.0 g) of the sample was ground for 24 h in a vibrating mill TI100 (Heiko Manufacturing Ltd). This machine is unique in that a single rod is used in place of the many balls widely used, making it easy to take out a sample of sticky nature from the pot. The pot and the rod are made of aluminium oxide. The free space of the pot is about 3 $cm^3$. The milling operation was stopped every 10 min and the pot was cooled with a fan to remove the heat arising from friction and impact between the pot and the rod. The surface temperature outside the pot was kept below 10 °C during the milling. The sample was kept in a dry nitrogen atmosphere throughout the milling. The complete amorphization of the sample was checked by x-ray powder diffraction. The LQG sample was prepared by plunging a TNB melt in a closed glass tube into liquid nitrogen. The cooling rate was roughly estimated to be 90 °C $min^{-1}$.

### *2.2. Adiabatic calorimetry*

The heat capacity of the LQG, GAS and crystal was measured with an adiabatic calorimeter described elsewhere [23]. The temperature was measured with a Rh–Fe resistance thermometer calibrated on the temperature scales EPT76 ($T < 30$ K) and IPTS68 ($T > 30$ K). The heat capacity difference caused by the conversion to the new temperature scale ITS90 [24] was estimated to be smaller than 0.05% over the temperature range 5–370 K. The imprecision of the heat capacity was within 0.3% in the temperature region where $T < 15$ K, 0.1% for 15 K $< T <$ 30 K, and 0.05% for $T > 30$ K.

The amount of the sample loaded in the cell was 2.259 45 g ($=4.9486\times10^{-3}$ mol) for the LQG, 1.410 06 g ($=3.0883\times10^{-3}$ mol) for the GAS and 2.268 17 g ($=4.9677\times10^{-3}$ mol) for the crystal. Helium gas (2 Torr at room temperature) was charged into the dead space of the cell ($\simeq$3 $cm^3$) to obtain good thermal contact between the cell and the sample. The temperature range of the measurement was between 5 and 370 K for the LQG and crystal. For the GAS accurate values of the heat capacity could not be obtained below 9 K because of the effect of the adsorption of the conduction gas (He) on the surface of the fine particles

of the GAS sample. The temperature step of the heat capacity measurement was about 0.5 K at the lowest temperature and increased progressively up to about 3 K with the increase of temperature.

## 3. Results

### *3.1. Heat capacities*

The molar heat capacities of the LQG, GAS and crystalline samples of TNB are collected together in tables 1, 2 and 3, respectively. They are also plotted in figure 1 as the open circles, closed circles, and triangles, respectively. The inset shows an enlarged view of the heat capacities in the lowest-temperature region.

**Table 1.** Heat capacities of TNB (LQG). $R = 8.3145$ J K$^{-1}$ mol$^{-1}$.

| $T$ | $C_p$ | $T$ | $C_p$ | $T$ | $C_p$ | $T$ | $C_p$ | $T$ | $C_p$ | $T$ | $C_p$ |
|---|---|---|---|---|---|---|---|---|---|---|---|
| K | $R$ | K | $R$ | K | $R$ | K | $R$ | K | $R$ | K | $R$ |
| 5.85 | 0.558 | 28.30 | 7.209 | 70.82 | 16.56 | 132.66 | 27.37 | 208.46 | 42.18 | 300.61 | 62.65 |
| 6.27 | 0.638 | 29.59 | 7.658 | 74.00 | 17.12 | 136.10 | 27.98 | 213.10 | 43.15 | 306.45 | 64.62 |
| 6.98 | 0.801 | 31.00 | 7.921 | 77.36 | 17.73 | 139.54 | 28.61 | 217.76 | 44.17 | 312.35 | 66.03 |
| 7.95 | 1.043 | 32.77 | 8.401 | 80.83 | 18.32 | 143.00 | 29.24 | 222.46 | 45.16 | 318.31 | 67.63 |
| 8.91 | 1.310 | 34.70 | 8.913 | 84.26 | 18.92 | 146.45 | 29.88 | 227.20 | 46.17 | 324.36 | 69.17 |
| 9.88 | 1.592 | 36.76 | 9.434 | 87.69 | 19.50 | 149.94 | 30.52 | 231.97 | 47.22 | 330.49 | 70.91 |
| 10.88 | 1.891 | 38.86 | 9.947 | 91.14 | 20.10 | 153.68 | 31.23 | 236.77 | 48.27 | 336.68 | 73.26 |
| 11.90 | 2.214 | 41.10 | 10.46 | 94.61 | 20.72 | 157.99 | 32.04 | 241.61 | 49.33 | 342.83 | 78.91 |
| 13.07 | 2.586 | 43.36 | 10.99 | 98.10 | 21.34 | 162.37 | 32.88 | 246.48 | 50.38 | 348.72 | 89.27 |
| 14.33 | 2.986 | 45.64 | 11.49 | 101.62 | 21.94 | 166.83 | 33.74 | 251.38 | 51.46 | 354.66 | 90.53 |
| 15.66 | 3.401 | 47.98 | 12.00 | 105.11 | 22.55 | 171.36 | 34.62 | 256.17 | 52.53 | 360.66 | 91.46 |
| 17.02 | 3.837 | 50.54 | 12.58 | 108.58 | 23.15 | 175.96 | 35.53 | 261.30 | 53.69 | 366.72 | 92.41 |
| 18.51 | 4.314 | 53.22 | 13.16 | 112.04 | 23.74 | 180.64 | 36.47 | 266.74 | 54.94 | 372.57 | 93.26 |
| 20.17 | 4.836 | 55.94 | 13.71 | 115.49 | 24.34 | 185.38 | 37.43 | 272.23 | 56.24 | | |
| 21.89 | 5.369 | 58.79 | 14.28 | 118.92 | 24.94 | 190.20 | 38.40 | 277.79 | 57.49 | | |
| 23.58 | 5.883 | 61.79 | 14.88 | 122.36 | 25.54 | 194.78 | 39.33 | 283.41 | 58.79 | | |
| 25.25 | 6.358 | 64.92 | 15.47 | 125.79 | 26.15 | 199.31 | 40.26 | 289.09 | 60.15 | | |
| 26.87 | 6.798 | 67.83 | 16.01 | 129.22 | 26.75 | 203.87 | 41.21 | 294.82 | 61.54 | | |

### *3.2. The glass transition and crystallization*

Figures 2 and 3 show the temperature dependence of the heat capacities and the spontaneous temperature drift rates around the glass transition, respectively. The drift rate was taken at 10 min after each energy input. This time was long enough for thermal equilibration in the cell to be attained in the temperature region free from the relaxation phenomena.

As shown by open circles in figure 2, a large heat capacity jump ($\Delta C_p$ = 150 J K$^{-1}$ mol$^{-1}$) appeared at around 340 K in the LQG. An exothermic temperature drift, followed by an endothermic one, was also observed in the same temperature region as shown by open circles in figure 3. These anomalies are both distinctive features of the

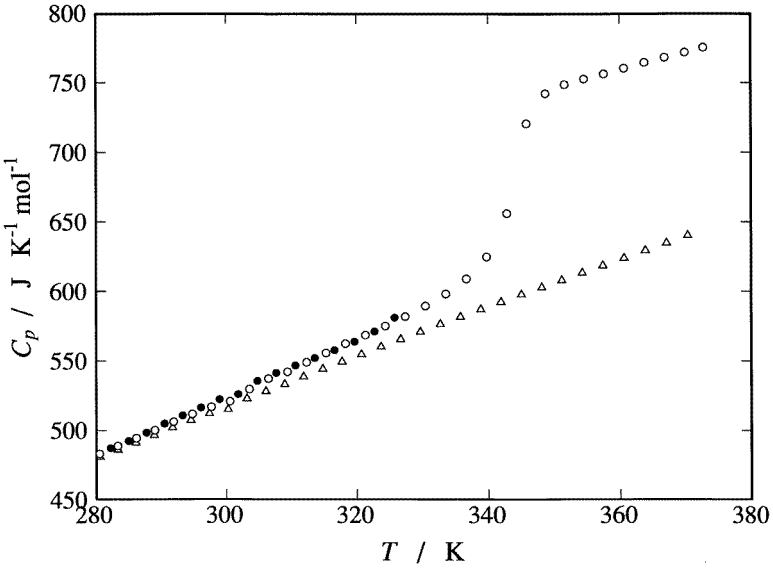


**Figure 2.** Heat capacities of TNB around the glass transition. Open circles: LQG; closed circles: GAS; triangles: crystal.

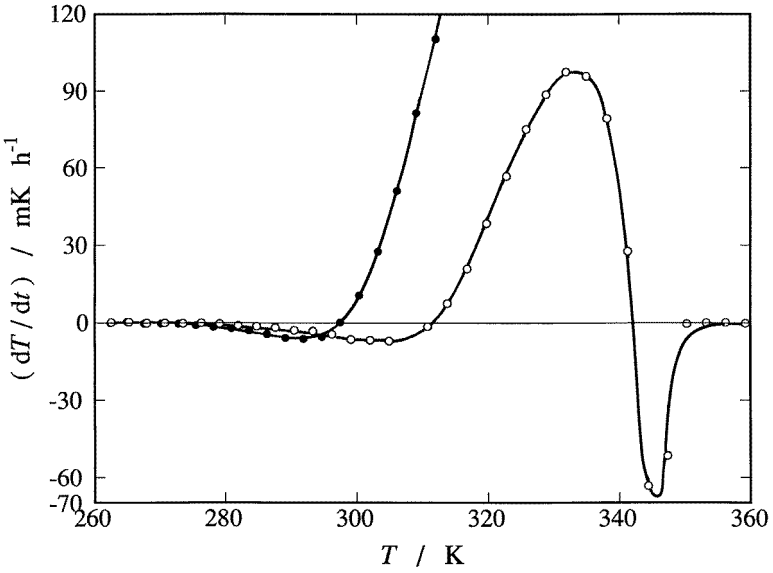


**Figure 3.** The spontaneous temperature drift rate of TNB observed during each equilibration period in the heat capacity measurement. Open circles: LQG; closed circles: GAS. The curves are drawn as guides to the eyes.

glass transition [25, 26]. The calorimetric glass transition temperature (342 K) was lower than $T_g$ determined by DSC (355 K) [9]. The crystallization of the LQG did not occur up to the highest temperature of this experiment (370 K).

The temperature dependence of the drift rate of the GAS (closed circles in figure 3)

was different from that of the LQG. An exothermic effect due to the enthalpy relaxation occurred from 300 K, which is about 10 K lower than in the case of the LQG, and a much larger exothermic effect due to crystallization began at around 320 K, which is about 25 K lower than $T_g$ for the LQG (342 K). The rate of the crystallization increased with increasing temperature and had a maximum ($dT/dt = 3900$ mK $h^{-1}$) at 342 K.

**Table 2.** Heat capacities of TNB (GAS). $R = 8.3145$ J $K^{-1}$ $mol^{-1}$.

| $T$ | $C_p$ | $T$ | $C_p$ | $T$ | $C_p$ | $T$ | $C_p$ | $T$ | $C_p$ | $T$ | $C_p$ |
|---|---|---|---|---|---|---|---|---|---|---|---|
| K | $R$ | K | $R$ | K | $R$ | K | $R$ | K | $R$ | K | $R$ |
| 9.87 | 1.662 | 41.77 | 10.67 | 85.06 | 19.18 | 136.32 | 28.00 | 197.27 | 39.85 | 266.38 | 54.87 |
| 11.35 | 2.128 | 44.13 | 11.20 | 87.55 | 19.62 | 139.82 | 28.62 | 201.45 | 40.72 | 271.61 | 56.16 |
| 13.13 | 2.666 | 46.53 | 11.70 | 89.22 | 19.90 | 143.34 | 29.28 | 205.67 | 41.59 | 276.92 | 57.32 |
| 14.95 | 3.225 | 48.95 | 12.28 | 90.91 | 20.22 | 146.87 | 29.94 | 209.93 | 42.48 | 282.31 | 58.62 |
| 16.73 | 3.786 | 51.38 | 12.79 | 94.31 | 20.80 | 150.33 | 30.59 | 214.22 | 43.40 | 287.79 | 59.96 |
| 18.47 | 4.348 | 53.84 | 13.33 | 97.75 | 21.38 | 153.86 | 31.24 | 218.55 | 44.34 | 293.35 | 61.43 |
| 20.18 | 4.878 | 56.38 | 13.85 | 101.25 | 21.96 | 157.50 | 31.95 | 222.91 | 45.27 | 298.99 | 62.83 |
| 22.19 | 5.511 | 58.97 | 14.39 | 104.79 | 22.55 | 161.25 | 32.66 | 227.31 | 46.21 | 304.74 | 64.41 |
| 24.20 | 6.116 | 61.64 | 14.89 | 108.38 | 23.16 | 165.10 | 33.38 | 231.74 | 47.19 | 310.61 | 65.76 |
| 26.29 | 6.699 | 64.40 | 15.43 | 112.03 | 23.77 | 168.99 | 34.16 | 236.21 | 48.15 | 316.62 | 67.08 |
| 28.58 | 7.372 | 67.25 | 15.92 | 115.53 | 24.37 | 172.92 | 34.93 | 240.71 | 49.13 | 322.72 | 68.71 |
| 30.84 | 7.940 | 70.11 | 16.48 | 118.98 | 24.97 | 176.89 | 35.72 | 245.25 | 50.12 | 325.80 | 69.90 |
| 32.96 | 8.533 | 72.90 | 17.00 | 122.43 | 25.54 | 180.89 | 36.51 | 249.82 | 51.11 | | |
| 35.11 | 9.119 | 75.83 | 17.54 | 125.89 | 26.15 | 184.93 | 37.32 | 252.12 | 51.63 | | |
| 37.28 | 9.648 | 78.87 | 18.07 | 129.35 | 26.76 | 189.01 | 38.15 | 256.21 | 52.52 | | |
| 39.46 | 10.14 | 82.02 | 18.66 | 132.83 | 27.37 | 193.12 | 39.00 | 261.25 | 53.66 | | |

The heat capacity of the crystal was measured using the sample obtained by annealing the GAS at around 360 K for 17 h. As shown in figure 2, the crystal exhibited no thermal anomaly in the glass transition region, indicating that the crystallization was complete.

### *3.3. Low-temperature heat capacity*

Figures 1 and 2 show that the heat capacities of the LQG (open circles) and GAS (closed circles) were 0.5–1% larger than those of the crystal (triangles) as frequently observed in glass-forming materials. To magnify the heat capacity difference between the GAS and LQG, heat capacities of the GAS and LQG relative to the smoothed heat capacity curve of the crystal are plotted in figure 4. The heat capacity of the GAS was the same as that of the LQG between 30 and 325 K. In the low-temperature region below 30 K, however, the heat capacity of the GAS was significantly larger than that of the LQG (1–4% of the total heat capacity of the GAS and 8–19% of the difference between the crystal and GAS). The origin of this difference will be discussed in section 4.3.

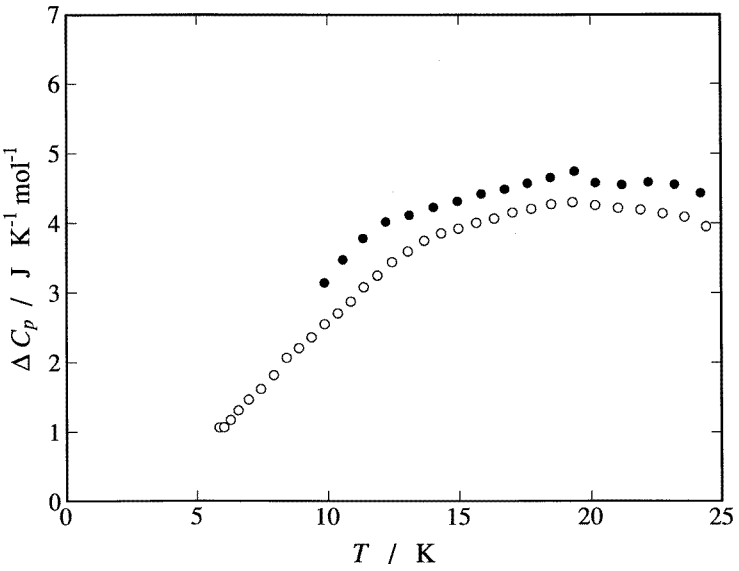


**Figure 4.** The heat capacity difference between LQG and crystal (open circles) and that between GAS and crystal (closed circles).

## 4. Discussion

### *4.1. Configurational enthalpy*

In the temperature region where the exothermic effect was observed in the heat capacity measurement, the sample was relaxing towards the equilibrium undercooled liquid via release of the excess enthalpy. This enthalpy corresponds to the configurational change of TNB molecules. The temperature and time dependence of the configurational enthalpy $H_c(T, t)$ was experimentally determined from

$$H_c(T, t) = \sum (dH_c/dt)\ \Delta t \tag{1}$$

where $dH_c/dt$ is the enthalpy relaxation rate. This quantity was evaluated by multiplying the spontaneous temperature drift rate by the heat capacity, including that of the sample cell. $\Delta t$ is the time between the midpoints of two successive energy inputs (about 30 min). The origin of $t$ is arbitrarily defined as a time at which the temperature is suitably low and no enthalpy relaxation occurs. The zero of $H_c(T, t)$ was taken at the terminal point of the relaxation (equilibrium liquid).

The configurational enthalpy of LQG ($H_c^{LQG}(T, t)$) could be determined with a uniquely assigned zero of the configurational enthalpy. This was possible because the sample reached the terminal point of the relaxation (equilibrium undercooled liquid) during the heat capacity measurement; $dH_c/dt$ reached zero at 342 K as shown in figure 3. In the case of the GAS, however, $H_c^{GAS}(T, t)$ could not be determined from equation (1) since the crystallization occurred before the equilibrium point was reached and so the starting point of the relaxation ($H_c^{GAS}(0, 0)$) could not be obtained. We therefore took $H_c^{LQG}(0, 0)$ as the reference point and evaluated $H_c^{GAS}(0, 0) - H_c^{LQG}(0, 0)$ by comparing the crystallization enthalpies of the GAS and LQG at the fictive temperature ($T_{fic} = 347.9$ K) of the LQG. The fictive temperature of the LQG is defined as the temperature where the equilibrium liquid has the same enthalpy as the glassy state [27, 28].

**Table 3.** Heat capacities of TNB (crystal). $R = 8.3145$ J K$^{-1}$ mol$^{-1}$.

| $T$ | $C_p$ | $T$ | $C_p$ | $T$ | $C_p$ | $T$ | $C_p$ | $T$ | $C_p$ | $T$ | $C_p$ |
|---|---|---|---|---|---|---|---|---|---|---|---|
| K | $R$ | K | $R$ | K | $R$ | K | $R$ | K | $R$ | K | $R$ |
| 5.47 | 0.379 | 29.54 | 7.229 | 73.59 | 17.00 | 127.45 | 26.36 | 200.63 | 40.40 | 291.79 | 60.38 |
| 5.93 | 0.441 | 31.63 | 7.749 | 76.82 | 17.59 | 130.96 | 26.97 | 205.30 | 41.37 | 297.45 | 61.59 |
| 6.61 | 0.557 | 33.78 | 8.378 | 80.24 | 18.18 | 134.37 | 27.58 | 210.02 | 42.33 | 303.18 | 62.88 |
| 7.34 | 0.698 | 35.95 | 8.969 | 82.95 | 18.67 | 137.85 | 28.23 | 214.77 | 43.34 | 308.97 | 64.13 |
| 8.11 | 0.857 | 38.12 | 9.532 | 85.34 | 19.08 | 141.42 | 28.87 | 219.55 | 44.36 | 314.82 | 65.44 |
| 8.92 | 1.046 | 40.29 | 10.06 | 89.06 | 19.71 | 145.09 | 29.55 | 224.38 | 45.38 | 320.74 | 66.73 |
| 9.89 | 1.289 | 42.43 | 10.57 | 93.07 | 20.41 | 148.86 | 30.25 | 229.23 | 46.41 | 326.72 | 68.03 |
| 10.96 | 1.572 | 44.53 | 11.04 | 86.74 | 19.32 | 152.72 | 30.97 | 234.13 | 47.46 | 332.75 | 69.33 |
| 12.19 | 1.903 | 46.69 | 11.55 | 90.48 | 19.97 | 156.68 | 31.72 | 239.06 | 48.54 | 338.85 | 70.62 |
| 13.56 | 2.289 | 48.90 | 12.06 | 94.23 | 20.61 | 160.73 | 32.48 | 244.02 | 49.62 | 345.00 | 71.90 |
| 15.02 | 2.729 | 51.15 | 12.56 | 98.01 | 21.26 | 164.87 | 33.28 | 249.02 | 50.70 | 351.21 | 73.15 |
| 16.47 | 3.166 | 53.42 | 13.07 | 101.80 | 21.91 | 169.09 | 34.10 | 254.05 | 51.83 | 357.48 | 74.41 |
| 18.01 | 3.642 | 55.92 | 13.60 | 105.62 | 22.55 | 173.40 | 34.94 | 259.22 | 52.95 | 363.80 | 75.71 |
| 19.69 | 4.175 | 58.61 | 14.15 | 109.47 | 23.22 | 177.80 | 35.82 | 264.47 | 54.20 | 370.17 | 77.00 |
| 21.50 | 4.740 | 61.42 | 14.71 | 113.35 | 23.89 | 182.29 | 36.70 | 269.80 | 55.41 | | |
| 23.34 | 5.329 | 64.35 | 15.28 | 116.95 | 24.50 | 186.83 | 37.60 | 275.20 | 56.60 | | |
| 25.29 | 5.912 | 67.44 | 15.86 | 120.45 | 25.12 | 191.39 | 38.52 | 280.66 | 57.85 | | |
| 27.44 | 6.541 | 70.57 | 16.46 | 123.95 | 25.73 | 195.99 | 39.46 | 286.19 | 59.10 | | |

The crystallization enthalpy of the LQG ($\Delta_{cr}H^{LQG}(T_{fic})$) was not obtained directly from the present experiment because the crystallization did not occur up to the highest temperature of this study (370 K). Therefore, it was evaluated from the heat capacity and the enthalpy of fusion via the thermodynamic relation

$$\Delta_{cr}H^{LQG}(T_{fic}) = \Delta_{fus}H - \int_{T_{fic}}^{T_{fus}} (C_{liq} - C_{cryst})\, dT \tag{2}$$

where$\Delta_{fus}H$ (= 33.3 kJ mol$^{-1}$) and $T_{fus}$ (=456.3 K) are the enthalpy and the temperature of fusion, respectively. These quantities were determined by DSC [9] using the same sample. $C_{liq}$ and $C_{cryst}$ are the heat capacities of the liquid and crystal, respectively. These were determined in the present study below 370 K and extrapolated to $T_{fus}$ with straight lines. The uncertainty of $\Delta_{cr}H^{LQG}$, involved in extrapolations of $C_{liq}$ and $C_{cryst}$, was estimated to be less than 0.1 kJ mol$^{-1}$.

The crystallization enthalpy of the GAS ($\Delta_{cr}H^{GAS}(T_{fic})$) was directly and precisely evaluated using the present calorimetric data and the equation

$$\Delta_{cr}H^{GAS}(T_{fic}) = \int_{T_i}^{T_{fic}} \left(\frac{dE}{dT}\right)_{GAS} dT + \int_{T_{fic}}^{T_f} \left(\frac{dE}{dT}\right)_{cryst} dT - \sum_{T_i}^{T_f} \Delta E \tag{3}$$

where $(dE/dT)_{GAS}$ and $(dE/dT)_{cryst}$ are, respectively, the heat capacities of the GAS and crystal including the heat capacity of the sample cell, $T_i$ (=297.6 K) is the temperature at which the exothermic effect due to the enthalpy relaxation began, $T_f$ (=368.2 K) is the temperature at which the exothermic phenomena due to the crystallization ceased, and $\Delta E$

is the electrical energy which was supplied to the sample and cell for the heat capacity measurement. The uncertainty of $\Delta_{cr}H^{GAS}(T_{fic})$ was less than 0.01 kJ mol$^{-1}$.

$\Delta_{cr}H^{LQG}(T_{fic})$ and $\Delta_{cr}H^{GAS}(T_{fic})$ thus determined were 20.4±0.1 kJ mol$^{-1}$ and 20.82± 0.01 kJ mol$^{-1}$, respectively. The difference between these quantities ($0.4 \pm 0.1$ kJ mol$^{-1}$) corresponds to the difference between the configurational enthalpies of the GAS and LQG before the relaxation took place; i.e., $H_c^{GAS}(0,0) - H_c^{LQG}(0,0) = 0.4 \pm 0.1$ kJ mol$^{-1}$. The value of $H_c(T,t)$ of the GAS below the crystallization temperature (315 K) was obtained by subtracting the relaxed enthalpy from $H_c^{GAS}(0,0)$ by further use of equation (1).

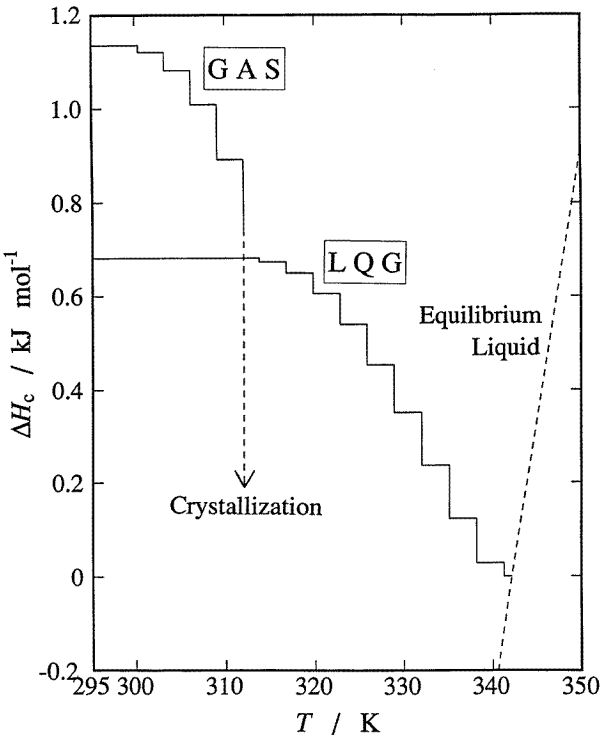


**Figure 5.** The temperature dependence of the configurational enthalpy of TNB.

Figure 5 shows the temperature dependence of the configurational enthalpies $H_c^{GAS}(T,t)$ and $H_c^{LQG}(T,t)$ obtained by the above calculation. The horizontal segments of the step-like lines represent the electrical heating which was assumed to take infinitesimally short intervals. The vertical ones represent the amount of enthalpy relaxed. The dotted curve smoothly rising to the right gives the configurational enthalpy of the equilibrium liquid. This curve was calculated on the basis of the heat capacity jump at the glass transition temperature. The origin of $H_c(T,t)$ was taken, as stated above, as being at the temperature at which the LQG sample reached the equilibrium state during the heat capacity measurement.

The total amount of the configurational enthalpy relaxed in the experiment was 1.1 kJ mol$^{-1}$ for GAS and 0.7 kJ mol$^{-1}$ for LQG. The value for GAS is 1.6 times larger than that for the LQG. The corresponding quantities in the case of TMCD were 2.0 kJ mol$^{-1}$ and 1.1 kJ mol$^{-1}$, respectively [12]. It is concluded from these results that the structure of the GAS is much more disordered and strained than that of the LQG. It is also noteworthy that the excess configurational enthalpy of the TNB GAS, which has

no intramolecular configurational change, is comparable with that of TMCD, which has a number of intramolecular configurations. This indicates that the main part of the excess enthalpy of the GAS is related to the intermolecular configurations and intermolecular interactions.

### *4.2. Anomalous crystallization in GAS*

Crystallization usually takes place at a temperature between that of the glass transition and that of fusion. In this temperature region, the Gibbs energy of the crystal is lower than that of the liquid and the structural relaxation time is short enough for the diffusion to take place as required for the crystallization. It is therefore unexpected that the crystallization of the GAS began below $T_g$ where the structural relaxation time is long ($\simeq 10^5$ s). The easy crystallization of the GAS was also observed in TMCD; the crystallization of the GAS occurred just above $T_g$ (345 K) while that of LQG was at 374 K. The crystallization below $T_g$ has also been found in vapour-deposited glasses (VDG) of simple hydrocarbons [29]. The common property for the GAS and VDG is that they have much larger enthalpy than the LQG [12, 30, 31]. We suppose that the highly disordered and strained structure of GAS may accelerate the rate of the diffusive motion of the molecule and cause the crystallization to occur below $T_g$. The crystalline nuclei left in the GAS sample may also be involved in the easy crystallization.

### *4.3. Low-energy excitation*

The excess heat capacities of the GAS and LQG in the lowest-temperature regions are associated with the low-energy excitations which are now believed to constitute a universal property of the amorphous materials [21]. The origin of the low-energy excitations has not yet been understood but it is most likely to be associated with disordered structure of the amorphous solid. The analysis presented above has revealed that the GAS is much more disordered and strained than the LQG. We suppose that the heat capacity difference between GAS and LQG ($C_p^{\mathrm{GAS}} \approx 1.01 \times C_p^{\mathrm{LQG}}$ at 15 K) was caused by the difference between the degree of disorder and strain in the structure of the GAS and that for LQG. Recently, it was reported that the magnitude of the low-energy excitation was reduced by annealing the amorphous metal and polymers around the glass transition [32, 33]; the annealing usually gave rise to short-range ordering in amorphous structure. The GAS may correspond to the sample before annealing.

## 5. Conclusion

From the calorimetric studies of TNB and TMCD [12], we conclude that the GAS has larger configurational enthalpy than the LQG, indicating that the structure of GAS is more disordered and strained than that of LQG. This can be related to the anomalous crystallization of GAS below the glass transition temperature. This may also be related to the large excess heat capacity due to the low-energy excitation of the GAS. X-ray and neutron diffraction studies would be useful for further investigation of the disordered and strained structure of the GAS in a more direct way. TNB should be a good candidate for use in such structural studies because of the intrinsic simplicity of its molecular shape.

## Acknowledgment

This work was supported by a Grant-in-Aid for Scientific Research No 06804032 from the Ministry of Education, Science and Culture.

## References

[1] Elliott S R 1984 *Physics of Amorphous Materials* (London: Longman)
[2] Zallen R 1983 *The Physics of Amorphous Solids* (New York: Wiley)
[3] Vogel W 1985 *Chemistry of Glass* (Columbus, OH: American Ceramic Society)
[4] Schwarz R B and Johnson W L (ed) 1988 *Solid State Amorphizing Transformations; J. Less-Common Met.* **140**
[5] Suzuki K and Wright A C (ed) 1992 *Structure of Non-crystalline Materials; J. Non-Cryst. Solids* **150** section 12
[6] Jimbo G, Kuwahara Y and Senna M (ed) 1992 *Proc. 4th Japan–Russia Symp. on Mechanochemistry* (Nagoya: Society of Powder Technology Japan)
[7] For example:
Hen Z 1993 *J. Phys.: Condens. Matter* **5** L337
Bernal M J, de la Cruz M M, Pareja R and Riviero J M 1995 *J. Non-Cryst. Solids* **180** 164
[8] For example:
Wright A C, Bachra B, Brunier T M, Sinclair R N, Gladden L F and Portsmouth R L 1992 *J. Non-Cryst. Solids* **150** 69
Bonnet J P, Boissier M and Gherbi A A 1994 *J. Non-Cryst. Solids* **167** 199
Fukunaga T 1995 *Physica* B **213+214** 518
[9] Tsukushi I, Yamamuro O and Matsuo T 1995 *Solid State Commun.* **94** 1013
[10] Tsukushi I, Yamamuro O and Suga H 1992 *Thermochim. Acta* **200** 71
[11] Tsukushi I, Yamamuro O and Suga H 1991 *J. Therm. Anal.* **37** 1359
[12] Tsukushi I, Yamamuro O and Suga H 1994 *J. Non-Cryst. Solids* **175** 187
[13] Plazek D J and Magill J H 1966 *J. Chem. Phys.* **45** 3038
[14] Magill J H and Ubbelohde A R 1958 *Trans. Faraday Soc.* **54** 1811
[15] Magill J H 1967 *J. Chem. Phys.* **47** 2802
[16] Fujara F and Petry W 1987 *Europhys. Lett.* **4** 921
[17] Ma R-J, He J-J and Wang C H 1988 *J. Chem. Phys.* **88** 1497
[18] Hofer K, Perez J and Johari G P 1991 *Phil. Mag. Lett.* **64** 37
[19] Bartsch E, Debus O, Fujara F, Kiebel M, Petry W, Sillescu H and Magill J H 1992 *Physica* B **180+181** 808
[20] Zemke K, Schmidt-Rohr K, Magill J H, Sillescu H and Spiess H W 1993 *Mol. Phys.* **80** 1317
[21] For example:
Phillips W A (ed) 1981 *Amorphous Solids—Low Temperature Properties* (Berlin: Springer)
Phillips W A 1987 *Rep. Prog. Phys.* **50** 1657
Buchenau U 1981 *Dynamics of Disordered Materials* ed D Richter, A J Dianoux, W Petry and J Teixeira (Berlin: Springer); 1993 *Phase Transitions and Relaxation in Systems with Competing Energy Scales* ed T Riste and D Sherrington (Dordrecht: Kluwer)
[22] Clapp D B and Morton A A 1936 *J. Am. Chem. Soc.* **58** 2172
[23] Yamamuro O, Oguni M, Matsuo T and Suga H 1987 *Bull. Chem. Soc. Japan* **60** 1269
[24] Goldberg R N and Weir R D 1992 *Pure Appl. Chem.* **64** 1545
[25] Suga H and Seki S 1974 *J. Non-Cryst. Solids* **16** 171
[26] Suga H 1985 *J. Chim. Phys. Phys.-Chim. Biol.* **82** 275
[27] Brawer S 1985 *Relaxation in Viscous Liquids and Glasses* (Columbus, OH: American Ceramic Society)
[28] Tool A Q and Eichli C G 1931 *J. Am. Chem. Soc.* **54** 491
[29] Takeda K, Oguni M and Suga H 1991 *J. Phys. Chem. Solids* **52** 991
[30] Hikawa H, Oguni M and Suga H 1988 *J. Non- Cryst. Solids* **101** 90
[31] Takeda K, Yamamuro O and Suga H 1995 *J. Phys. Chem.* **99** 1602
[32] Otomo T, Arai M, Shibata K, Mizuseki H and Suzuki K 1995 *Physica* B **213+214** 544
[33] Kanaya T, private communication